



Published in final edited form as:

*Liver Int.* 2015 April ; 35(4): 1133–1144. doi:10.1111/liv.12456.

## PROTECTIVE EFFECTS OF FXR ON HEPATIC LIPID ACCUMULATION ARE MEDIATED BY HEPATIC FXR AND INDEPENDENT OF INTESTINAL FGF15 SIGNAL

Johannes Schmitt<sup>#1</sup>, Bo Kong<sup>#2</sup>, Bruno Stieger<sup>3</sup>, Oliver Tschopp<sup>4</sup>, Simon M. Schultze<sup>4</sup>, Monika Rau<sup>1</sup>, Achim Weber<sup>5</sup>, Beat Müllhaupt<sup>6</sup>, Grace L. Guo<sup>#2</sup>, and Andreas Geier<sup>#1,6,§</sup>

<sup>1</sup> Division of Hepatology, Department of Medicine II, University Hospital Wuerzburg, DE-97080 Wuerzburg, Germany <sup>2</sup> Department of Pharmacology and Toxicology Ernest Mario School of Pharmacy Rutgers University Piscataway, NJ 08854, USA <sup>3</sup> Department of Clinical Pharmacology and Toxicology, University Hospital Zurich (USZ), CH-8091 Zurich, Switzerland <sup>4</sup> Division of Endocrinology, Diabetes, & Nutrition, University Hospital of Zurich, Zurich, Switzerland <sup>5</sup> Department of Pathology, Institute of Surgical Pathology, University Hospital Zurich (USZ), Zurich, Switzerland <sup>6</sup> Department of Gastroenterology & Hepatology, University Hospital Zurich (USZ), Zurich, Switzerland

# These authors contributed equally to this work.

### Abstract

**Background and Aims**—There is growing evidence that bile acids are involved in the regulation of triglyceride-, cholesterol-homeostasis and fat absorption. In this study organ-specific *Fxr* knockout mice were used to further investigate the influence of FXR in lipogenesis.

**Methods**—Liver- and intestine-specific *Fxr* knockout mice were fed a 1% cholesterol diet for 28 days. Histological examination of frozen tissue sections included Sudan III/H&E, BODIPY staining and LXR immunohistochemistry. Liver triglycerides, serum cholesterol, serum bile acids and nuclear LXR protein were measured. mRNA expression of several genes involved in bile acid-, cholesterol-homeostasis and lipogenesis was quantified by real-time PCR.

**Results**—Hepatic FXR deficiency contributes to lipid accumulation under 1% cholesterol administration which is not observed in intestinal *Fxr* knockout mice. Strong lipid accumulation, characterized by larger vacuoles could be observed in hepatic *Fxr* knockout sections, while intestinal *Fxr* knockout mice show no histological difference to controls. Additionally, those mice have the ability to maintain normal serum cholesterol and bile acid levels. Hepatic *Fxr* knockouts were characterized by elevated triglycerides and bile acid levels. Expression level of LXR was significantly elevated under control and 1% cholesterol diet in hepatic *Fxr* knockout mice and was

§**Corresponding author:** Andreas Geier, M.D., Division of Hepatology, Department of Medicine II, University Hospital Würzburg, Oberdürrbacherstrasse 6, D-97080 Würzburg, Germany. Phone: ++49 931 201 40021, FAX: ++49 931 201 640201  
geier\_a2@medizin.uni-wuerzburg.de.

Conflict of interest:

There is no conflict of interests

followed by concomitant lipogenic target gene induction such as *Fas* and *Scd-1*. This protective FXR effect against hepatic lipid accumulation was independent of intestinal *Fgf15* induction.

**Conclusions**—These results show that the principal site of protective bile acid signalling against lipid accumulation is located in the liver since the absence of hepatic but not intestinal FXR contributes to lipid accumulation under cholesterol diet.

### Keywords

FXR; bile acids; NAFLD; Lipogenesis

## Introduction

Nonalcoholic fatty liver disease (NAFLD) represents a chronic liver disease and cofactor in other metabolic diseases with worldwide growing incidence (1). This syndrome caused by Western diet is characterized by accumulation of lipids in the liver. The prevalence of NAFLD in the general population is 10 to 24% and includes a clinical spectrum of disease ranging from simple steatosis to non-alcoholic steatohepatitis (NASH) and finally advanced fibrosis and cirrhosis (2-5). Despite the high frequency of NAFLD the pathogenesis of this disease is still poorly understood and no satisfying long-term therapy exists to date.

Several studies point out, that bile acids are involved in the regulation of triglyceride and glucose metabolism, next to their well characterized functions in cholesterol homeostasis, fat absorption and control of their own synthesis (6-8). The farnesoid X receptor (FXR) as the nuclear bile acid receptor, is activated by bile acids as ligands and represents an intracellular bile-acid sensor which is the key regulator of bile acid homeostasis (9). Activated FXR suppresses via small heterodimer binding partner (SHP) the bile acid synthesis by down-regulation of *CYP7A1*, the enzyme that catalyzes the first and rate-limiting step in bile acid synthesis (10). The FXR-induced fibroblast growth factor (FGF) 15 signalling pathway, originating in the small intestine, is incorporated in the regulatory circle of bile acid homeostasis. This pathway in turn represses hepatic *CYP7A1* through its binding to the FGF receptor 4 (FGFR4) and subsequent activation of SHP (6, 11).

There is a growing evidence confirming a functional interaction between these bile acid-dependent FXR-pathways and hepatic triglyceride metabolism since bile acid-feeding in different models of hypertriglyceridemia decreased *de novo* lipogenesis through down-regulation of sterol regulatory element binding protein-1c (SREBP-1c) resulting in reduced plasma triglycerides (12, 13). In line with these observations, deficiency of FXR *in vivo* causes severe alterations in systemic lipid metabolism with increased serum triglycerides, cholesterol (primarily HDL) levels and free fatty acids (14-16). Hence, *Fxr*<sup>-/-</sup> mice develop a fatty liver (14, 16) which is severely aggravated when fed a 1% cholesterol diet (16). In support of a beneficial role of FXR in this regard, several studies in rodent models of fatty liver disease (db/db and ob/ob mice) show a significant improvement of insulin sensitivity and a reduction of hepatic lipid accumulation when treated with the synthetic FXR-specific agonist GW4064 (17, 18).

The fact that GW4064 is featured by a poor bioavailability raises the obvious question, whether hepatic or intestinal activated FXR has a protective effect against accumulating lipids in the liver. In this regard, it is also unclear whether bile acid retention and subsequent hepatic FXR activation in fatty livers represents a causal event in the pathogenesis or rather an attempt of adaptation (19, 20). Following these pertinent questions we studied organ-specific liver ( $\Delta L$ ) and intestinal ( $\Delta IE$ ) *Fxr* knockout mice under a 1% cholesterol diet. Our results demonstrate that the organ-specific absence of FXR in the liver leads to lipid accumulation, which is independent of FXR and FGF15 signalling in the intestine.

## Material and Methods

### Animal model

Liver-specific (*Fxr*  $\Delta L$ ) and intestine-specific (*Fxr*  $\Delta IE$ ) *Fxr* knockout mice were generated as previously described (21). Mice were housed under standard 12 hr light and 12 hr dark cycle. All the experiments were performed with age-matched male *Fxr*  $\Delta L$  and *Fxr*  $\Delta IE$  mice, as well as *Fxr flox/flox* (f/f) littermates without albumin-cre or villin-cre recombinase transgene used as controls (n=4 from each group). All mice have been cross-bred with C57BL/6J mice for 8 to 10 generations with congenic test confirming background purity. All diets were based upon a standard AIN-93G rodent diet containing 58.6% carbohydrate, 18.1% protein, 7.2% fat, 5.1% fiber, 3.4% ash, and 10% moisture (control diet). Experimental diets consisted of the control diet supplemented with 1% cholesterol (w/w) according to the original description of *Fxr*-null mice by Sinal et al. (16). Prior to the administration of special diets for a duration of 28 days, mice were fed standard rodent chow and water ad libitum.

From the scarified animals serum was taken and tissues were snap-frozen in liquid nitrogen and stored at  $-80^{\circ}\text{C}$  until further use. The animals received humane care and the study protocols were approved by the local Government's Animal Care Committee.

### Histology

To examine the accumulation of hepatic lipids, frozen liver sections were stained either with Sudan III and Hematoxylin or BODIPY (Invitrogen, Basel, Switzerland). For BODIPY staining frozen liver sections were fixed in 10% formaldehyde, washed twice with PBS and incubated with 1 $\mu\text{g/ml}$  BODIPY 493/503 (Invitrogen, #D-3922) in 150mM NaCl for 20 minutes at room temperature. After incubation slides were washed twice with PBS and mounted with "Vectashield with DAPI" (Vectorlaboratory, Cat. No. H-1200). Images were acquired with a Zeiss Z1 microscope and processed with AxioVision 4.7.1. software from Carl Zeiss (Jena, Germany). The obtained data were processed by using Photoshop CS3 Extended (Adobe Systems, San Jose, CA).

### Immunohistochemistry

Immunohistochemistry procedure was described before (22). Cryosections were fixed for 5 min in PBS containing 1% formaldehyde and were permeabilized for 10 min in PBS containing 0.1% Triton X-100. After blocking for 1h with PBT (PBS containing 1.5%BSA and 0.1% Tween 20), specimens were incubated with LXR (LS-B3526) antibody (LifeSpan

Bioscience, Seattle, US) for 1h. Then specimens were washed twice in PBS, and bound antibodies were detected with corresponding secondary antibodies (Invitrogen). DNA was visualized with the fluorochrome DAPI (Sigma-Aldrich, St. Louis, US). After a final washing in PBS, the cells were embedded in Kaisers glycerol gelatine (Merck, Darmstadt, Germany). Ominofocal analyses were done with a Biorevo BZ-9000 (Keyence, Neu-Isenburg, Germany). The obtained data were processed by using Photoshop (Adobe Systems, San Jose, CA).

### Serum and tissue chemistry

Serum cholesterol was measured using a serum multiple biochemical analyzer (Ektachem DTSCII; Johnson & Johnson Inc., Rochester, NY). For glucose levels a glucose meter (FreeStyle; Disetronic Medical System AG, Burgdorf, Switzerland) was used. To measure triglyceride content in the liver, lipids were extracted from approximately 30mg of tissue by homogenization in 700µl of acetone (23). For liver cholesterol measurement 25mg of liver tissue was used in the Cholesterol/Cholesteryl Ester Quantitation Kit II (BioVision, K623-100). The procedure was performed according to the manufacturer's instructions. Homogenates were centrifuged twice for 5 minutes at full speed to remove cell debris. Triglyceride concentrations were measured using TRIG kit (diatools, Villmergen, Switzerland) according to manufacturer's instructions. Serum bile acids were measured by radioimmunoassay using a Bile Acid RIA Kit (MP Biomedicals, Ilkirch, France) according to the manufacturer's specifications.

### Western Blotting

Similar amounts of total protein extract were separated by SDS-PAGE, transferred to nitrocellulose membrane and probed with SREBP-1 antibody (LifeSpan BioScience, LS-C30185, Seattle, USA). After incubation with species-specific HRP-conjugated secondary antibody (Jackson ImmunoResearch Laboratories, Suffolk, UK) immune complexes were detected using Clarity™ Western ECL Substrate (Biorad, Munich, Germany). Densitometric quantification of Western blots was performed using Adobe Photoshop CS3.

**Quantification of nuclear LXR Protein**—25mg of liver tissue was used to isolate nuclear fractionations using the NE-PER Nuclear Extraction Reagents kit (Thermo Fisher Scientific) according to the manufacturer's protocol. Total protein concentration was measured using the Pierce® BCA Protein Assay Kit. Nuclear LXR protein was determined using ELISA Kit for Liver X Receptor Alpha (E92044Mu Usen). LXR protein was normalized against total nuclear protein content.

**mRNA isolation and real-time RT-PCR**—Total RNA was isolated from liver and ileum by using RNeasy Mini Kit (Qiagen, Valencia, CA) according to manufacturer's instructions. mRNA was reverse-transcribed to cDNA using the High Capacity cDNA Reverse Transcription Kit (Applied Biosystems, Mannheim, Germany). Real-time PCR was performed using ABI TaqMan probes and PCR-Primers in combination with TaqMan® Fast Universal PCR Master Mix or FAST SYBR Green PCR Master Mix (Applied Biosystems), respectively (20). For primer design Primer Express software (Applied Biosystems; Foster City, CA) was used. Primers sequences used for gene expression analysis are listed in table

1. For *Abcg5* and *Abcg8* commercially available TaqMan assays had been used on an Applied Biosystems 7900HT Fast Real-Time PCR System (Applied Biosystems, Foster City, USA).

**Statistical analysis**—The significance of differences between the experimental groups was determined by Mann-Whitney U-test. (GraphPad Software Inc., CA, USA). Probability values less than 0.05 were considered significant. Data represented the mean  $\pm$  SEM.

## RESULTS

### Liver specific FXR deficiency promotes lipid accumulation

Systemic FXR deficiency leads to dysregulation of bile acid homeostasis and lipid metabolisms (16), but the particular contribution of hepatic and intestinal FXR to lipid metabolism is not completely clarified yet. To investigate the organ-specific influence of FXR on lipid metabolism, organ-specific *Fxr*<sup>-/-</sup> mice with deletion of either hepatic ( $\Delta$ L) or intestinal ( $\Delta$ IE) FXR were put on 1% cholesterol diet (1%CD) for 28 days.

Under control diet the organ-specific *Fxr* knockout mice showed unaltered liver tissue in sudan III and hematoxylin staining, and show no histological difference from *flox/flox* controls (Figure 1A). After 28 days of 1% cholesterol diet, small lipid vacuoles were present in the livers of *flox/flox* controls. This phenotype could be also observed in intestinal ( $\Delta$ IE) *Fxr* knockout mice. In contrast to this mild lipid accumulation, a prominent lipid accumulation, characterized by larger vacuoles could be observed in hepatic ( $\Delta$ L) *Fxr* knockout. The pattern of lipid accumulation was verified with BODIPY staining, a lipophilic fluorescent agent (Figure 1). In line with the histological phenotype, an increased hepatic triglyceride concentration could be measured in ( $\Delta$ L) *Fxr* knockout animals under control diet (*f/f* 5.8 $\pm$ 1.1  $\mu$ mol/g vs.  $\Delta$ L 19.9 $\pm$ 4.0  $\mu$ mol/g; P=0.015) and under 1%CD feeding (*f/f* 34.8 $\pm$ 4.4  $\mu$ mol/g vs.  $\Delta$ L 58.2 $\pm$ 13.6  $\mu$ mol/g; P=0.155) compared to *flox/flox* controls under respective diet (Figure 2A). In contrast, no increase of hepatic triglyceride content could be observed in ( $\Delta$ IE) *Fxr* knockout mice compared to *flox/flox* controls for both forms of diet.

### Hepatic *Fxr* knockout mice are characterized by altered serum bile acids and cholesterol concentration

To characterize the physiologic consequence of 1% cholesterol feeding in the organ-specific *Fxr* knockout mice and their *flox/flox* littermates, serum bile acids, serum cholesterol, total liver cholesterol and serum glucose concentrations were quantified.

*Flox/flox* (*f/f*) littermates without albumin-cre or villin-cre recombinase transgene showed identical serum characteristics. The cholesterol levels in ( $\Delta$ L) *Fxr* knockout mice under control diet were significantly elevated compared to *flox/flox* controls ( $\Delta$ L 123 $\pm$ 16.6 mg/dl vs. *f/f* 65.5 $\pm$ 7.1 mg/dl, P=0.019) and ( $\Delta$ IE) *Fxr* knockouts. Under 1% cholesterol chow, ( $\Delta$ IE) *Fxr* knockout animals showed a serum cholesterol level that was comparable with *flox/flox* controls, while ( $\Delta$ L) knock out mice were characterized by significantly higher cholesterol levels (*f/f*, 105.5 $\pm$ 10.4 mg/dl vs.  $\Delta$ L, 244.5 $\pm$ 22.8 mg/dl; P=0.001;  $\Delta$ IE, 111.75 $\pm$ 5.25 mg/dl) (Figure 2B). In line with these findings was a significant higher total

liver cholesterol level under standard diet (*f/f*, 62.4±3.28 mg/dl vs.  $\Delta$ L, 89.6±3.08mg/dl;  $P=0.0286$ ;  $\Delta$ IE, 76.1±11.7 mg/dl) (Figure 2E). Total serum bile acids were slightly increased in ( $\Delta$ L) *Fxr* knockout mice compared to *flox/flox* controls and ( $\Delta$ IE) *Fxr* knockouts, irrespective of the diet (control diet: *f/f*, 3.1±0.4  $\mu$ M/l vs.  $\Delta$ L, 7.5±1.3  $\mu$ M/l;  $P=0.021$ ; trend for 1%CD: *f/f*, 5.5±1.1  $\mu$ M/l;  $\Delta$ L, 10.0±3.4  $\mu$ M/l;  $P=0.251$ ) (Figure 2C). The glucose levels of all experimental groups were comparable to *flox/flox* controls under control diet, with the exception of ( $\Delta$ L) *Fxr* knockout mice which showed a slight but significant elevation under 1% cholesterol feeding (*f/f*, 108.6±14.6 % vs.  $\Delta$ L, 140.6±8.9 %;  $P=0.017$ ).

### Gene expression analysis of FXR targets and genes related to bile acid and cholesterol homeostasis

To obtain mechanistic insight into the pathophysiological events underlying hepatic lipid accumulation under organ-specific *Fxr* knockout conditions, expression of FXR target genes particularly those involved in bile acid, cholesterol and lipid homeostasis were analyzed.

To confirm the genotype of the different experimental group's functional FXR transcripts were undetectable in the respective organs of mice with hepatic ( $\Delta$ L) or intestinal ( $\Delta$ IE) *Fxr* deletion (Figure 3A and 3B). As known from the literature (21) a minor but not significant decrease in SHP mRNA could be observed in hepatic ( $\Delta$ L) *Fxr* knockout mice under control diet. *Cyp7a1* was significantly upregulated in hepatic ( $\Delta$ L) *Fxr* knockout mice under control diet ( $\Delta$ L, 293.1±98.6% vs. *f/f*, 100±13.1%;  $P=0.0286$ ). No significant change in *Cyp7a1* mRNA expression could be observed in ( $\Delta$ IE) *Fxr* knockout mice under standard diet (Figure 3A).

The bile salt export pump (BSEP), another target gene of FXR was significantly down-regulated in ( $\Delta$ L) *Fxr* knockout mice irrespective of the diet (control diet:  $\Delta$ L 45.8±5.7 %,  $P=0.0079$ ; 1%CD:  $\Delta$ L 29.6±8.2 %,  $P=0.0043$ ), while no such change was detected in *flox/flox* controls or ( $\Delta$ IE) *Fxr* knockout mice (Figure 3A).

As an intestinal FXR target gene and as prove of principle control for the organ-specific knock down, the ileal bile acid binding protein (IBABP) was investigated. As expected, functional transcripts were only undetectable in  $\Delta$ IE mice, irrespective of the diet (Figure 3B).

To investigate the influence of organ-specific *Fxr* deletion on intestinal FGF15 signalling and the observed lipid accumulation, FGF15 mRNA was quantified in ileal tissue. 1% cholesterol feeding leads to an induction of FGF15 in *flox/flox* controls and ( $\Delta$ L) *Fxr* knockout mice which could not be demonstrated in ( $\Delta$ IE) mice characterized by intestinal FXR deficiency (Figure 3B).

Since ( $\Delta$ L) *Fxr* knockout animals were characterized by an elevated serum and liver cholesterol level under standard chow, we analyzed the expression of the nuclear oxysterol receptor LXR that serves as the key regulator of cholesterol homeostasis. In line with respective serum and liver cholesterol levels, there was no significant change in hepatic LXR mRNA expression in ( $\Delta$ IE) *Fxr* knockouts compared to *flox/flox* controls, irrespective of the diet, whereas a significant LXR mRNA elevation could be observed in ( $\Delta$ L) *Fxr*

knockout animals (control diet: *f/f*, 100±9.3% vs.  $\Delta$ L, 144.7±9.7%,  $P=0.016$ ; 1%CD: *f/f*, 105.0±6.3% vs.  $\Delta$ L, 153.9±9.2,  $P=0.009$ ) (Figure 4A). To verify the transcriptional effect of LXR, the LXR protein concentration was measured in nuclear fractions. A significant increase in LXR nuclear protein could be observed in ( $\Delta$ L) *Fxr* knockout animals under standard diet and with a clear trend under 1% cholesterol diet (control diet: *f/f*, 100±18.0% vs.  $\Delta$ L, 281.4±63.7%,  $P=0.029$ ; 1%CD: *f/f*, 189.7±34.1% vs.  $\Delta$ L, 433.4±97.2,  $P=0.0571$ ) (Figure 4B). Additionally, an increased nuclear localization could be visualized in animals under 1% cholesterol diet. Consistent with the mRNA data, an increased localisation of LXR, could be observed in ( $\Delta$ L) *Fxr* knockout animals under standard diet, while there was a lower expression documented in *flox/flox* littermates under the same treatment (Figure 4C).

As the rate limiting enzyme in cholesterol synthesis, hydroxymethylglutaryl-Coenzyme A reductase (HMGCoAR) was significantly decreased in feedback to cholesterol overload (1%CD). Interestingly, a significant increase of HMGCoAR could be measured in ( $\Delta$ L) *Fxr* knockout mice under control diet which parallels the elevated serum cholesterol levels in these mice ( $\Delta$ L 130.3±4.5% vs. *f/f* 100±9.8%,  $P=0.023$ ) (Figure 4D). Under 1% cholesterol feeding a significant mRNA increase of the ABC sterol transporters *Abcg5* and *Abcg8* was observed in all experimental groups whereas no such increase was observed under control diet (Figure 4E+F).

### Gene expression analysis of genes related to lipid homeostasis

To examine the consequences of LXR activation, direct or indirect target genes involved in the lipogenesis were analyzed. Nuclear SREBP-1c protein expression was found to be elevated in both wildtype and ( $\Delta$ L) *Fxr* knockout animals under cholesterol diet. Notably, nuclear SREBP-1c was also increased in ( $\Delta$ L) *Fxr* knockout mice under standard diet (Figure A, B). In line with these findings, fatty acid synthase (*Fas*) was significantly upregulated in ( $\Delta$ L) *Fxr* knockout mice under control diet compared to *flox/flox* controls ( $\Delta$ L, 184.2±34.4% vs. *f/f*, 100±13.5%,  $P=0.016$ ) which was less pronounced under 1% cholesterol (Figure 5C).

Stearoyl CoA Desaturase-1 (SCD-1), which is required for synthesis of unsaturated fatty acids, was significantly elevated in ( $\Delta$ L) *Fxr* knockout mice compared to respective *flox/flox* controls under both control diet and 1% cholesterol (control diet: *f/f* 100±15.0% vs.  $\Delta$ L 239.5±58.0%,  $P=0.032$ ; 1%CD: *f/f* 223.8.4±37.3% vs.  $\Delta$ L 444.8±91.0%,  $P=0.035$ ) (Figure 5 D). No difference in SCD-1 expression could be observed in ( $\Delta$ IE) *Fxr* knockout mice to *flox/flox* controls for both diets.

The same pattern of gene expression was detected for patatin-like phospholipase domain containing 3 gene (PNPLA3), a lipid acyl hydrolase which plays a role in lipid remodelling. An increase of PNPLA3 mRNA was detected in ( $\Delta$ L) *Fxr* knockout mice compared to respective *flox/flox* controls irrespective of the diet (control diet: *f/f* 100±27.6 % vs.  $\Delta$ L 733.8±227.4%,  $P=0.0159$ ; 1%CD: *f/f* 266.0±113.9 % vs  $\Delta$ L 754.4±231.7% $P=0.0411$ ) (Figure 5 E).

## DISCUSSION

Bile acids play a central role in the complex regulation of triglyceride metabolism and cholesterol homeostasis. The absence of the bile acid receptor FXR *in vivo* has profound consequences on systemic lipid metabolism since respective knockout mice are characterized by increased serum free fatty acids, triglycerides and cholesterol (6-8, 10, 11). A direct functional link between bile acid-dependent FXR-activation and triglyceride metabolism has been established in bile acid-feeding studies using different models of hypertriglyceridemia (12, 13). The fact that beneficial effects of the FXR-ligand GW4064 against accumulating lipids in the liver can be observed despite a poor bioavailability suggests rather the involvement of intestinal FXR signals than direct hepatic effects. However, the underlying mechanism has not been clarified thus far. To address this relevant question in detail, organ-specific *Fxr*<sup>-/-</sup> mice with deletion of either hepatic or intestinal FXR were subjected to a 1% cholesterol diet, which has been shown to aggravate the development of fatty liver in systemic *Fxr*<sup>-/-</sup> mice (6).

The major findings of this study are the following:

- i. The principal site of protective FXR signalling against lipid accumulation is located in the liver. Absence of hepatic FXR ( $\Delta L$ ) contributes to lipid accumulation under 1% cholesterol diet which is not observed in intestinal ( $\Delta IE$ ) *Fxr* knockout mice and *flox/flox* controls.
- ii. Similarly, the ability of intestinal ( $\Delta IE$ ) *Fxr* knockout mice and controls to maintain normal serum cholesterol and bile acid levels under cholesterol diet is absent in mice with hepatic ( $\Delta L$ ) *Fxr* knockout.
- iii. Hepatic ( $\Delta L$ ) *Fxr* knockout mice are characterized by elevated liver x receptor (LXR) expression, increased nuclear protein localization and concomitant induction of lipogenic target genes such as *Scd-1* and *Fas*.
- iv. Of note, protective FXR effects against hepatic lipid accumulation under 1% cholesterol diet are independent of intestinal Fgf15 induction.

Hepatic cholesterol homeostasis requires a cascade of enzymatic reactions in the biotransformation of bile acids with CYP7A1 as the rate-limiting enzyme followed by their excretion through the canalicular transport systems including Bsep (10, 24). Systemic disruption of the *Fxr* gene leads to the aberrant cholesterol and lipid homeostasis which has been attributed to defects in bile acid transport with decreased Bsep expression (16). Whereas wildtype animals have the ability to maintain low hepatic cholesterol concentrations under high cholesterol intake, FXR deletion leads to the accumulation of intrahepatic and serum cholesterol despite increased Cyp7a1 (16). The absence of FXR signalling in FXR deleted mice is accompanied by cholesterol accumulation compared to wildtype mice which is even aggravated by additional cholesterol feeding (16). In accordance with these data from systemic *Fxr*<sup>-/-</sup>, the same increase in Cyp7a1 expression in combination with decreased Bsep can be observed in  $\Delta L$  *Fxr* mice in the present study. In this context, bile acid retention due to reduced bile acid transporter expression as observed in various rodent models of fatty liver (19, 20) may be rather protective than contributing to



cholesterol accumulation as far as FXR expression and signalling is intact. Indeed, recent pilot data from *Bsep*  $-/-$  mice fed a methionine-choline-deficient diet clearly indicate that fat accumulation and inflammation is even ameliorated upon retention of CDCA and CA in these animals both known as FXR agonists (C.D. Fuchs, T. Claudel, E. Halilbasic, T. Stojakovic, and M. Trauner, presented at the 48<sup>th</sup> Annual Meeting of the European Association for the Study of the Liver, Amsterdam, The Netherlands, 24-28 April 2013) (25). In accordance with previous data SHP is not induced in 1% cholesterol diet animals since it has been shown that SHP induction is repressed by free fatty acids (FFA) in NAFLD patients and hepatoma cells (28). Besides the role of FXR in cholesterol homeostasis, FXR represents a negative regulator of the oxysterol receptor LXR (33). LXR is activated by oxidized derivatives of cholesterol (oxysterols) and plays a crucial role in regulating the expression of genes involved in cholesterol homeostasis and lipid metabolism (29, 30). Under physiological conditions, activation of FXR and subsequently SHP will eliminate a stimulatory effect of LXR on the CYP7A1 promoter (Shang Q *Am J Physiol* 2007). As a mechanistic clue from our study CYP7A1 mRNA (and bile acid levels) are increased even under standard diet, in animals where LXR activation occurs solely by the absence of FXR ( $\Delta L$  *Fxr* mice). This was independent of SHP expression which remains at baseline.

HMGCoAR is the rate limiting enzyme in cholesterol homeostasis and negatively controlled by intracellular cholesterol (31, 32). In line with the observation that FXR agonists downregulate HMGCoAR, ( $\Delta L$ ) *Fxr* knockout animals are characterized by an elevated *HMGCoAR* mRNA expression in our study which might contribute to increased serum cholesterol levels without cholesterol overload under standard chow.

Besides the regulation of cholesterol homeostasis LXR activation increases the expression of genes involved in fatty acid biosynthesis (lipogenesis), and raises plasma triglyceride levels (hypertriglyceridemia) (34). Functionally, the induction of the lipogenic genes *Scd-1* and *Fas* upon administration of a synthetic LXR agonist contributes to massive hepatic steatosis in mice (34). In line with the concept that accumulating cholesterol leads to LXR activation and increased expression by autoactivation of the gene (35), hepatic *Fxr* knockout mice in our study are characterized by elevated LXR expression and elevated SREBP-1c. LXR induces SREBP-1c gene transcription and induce de novo lipogenesis (36). The principal mechanism for SREBP-1c regulation involves control of its nuclear localization and binding to sterol regulatory elements in promoter regions of specific genes. SREBP-1c is regulated by posttranslational proteolytic processing in the Golgi apparatus and transported to the nucleus (nuclear SREBP-1c) (36, 37). In line with increased LXR expression, hepatic *Fxr* knockout mice under control diet in our study show an elevated nuclear localization of SREBP-1c, resulting in concomitant induction of lipogenic target genes including *Scd-1* and *Fas* under control diet. A less pronounced up-regulation of *Fas* under cholesterol feeding is in line with a previously observed *Fas* mRNA down-regulation in cholesterol-fed rodents (38). In contrast, SCD-1 which is prominently induced under cholesterol feeding seems to be even more important for lipid accumulation under these conditions. In turn, LXR induction and concomitant induction of *Scd-1* is absent in intestinal *Fxr* knockout mice which nicely correlates with the absent lipid accumulation in these livers.

The principal site of protective FXR signalling against lipid accumulation has not been clear so far. From previous studies under standard diet, it appeared that treatment with the FXR agonist GW4064 significantly represses hepatic Cyp7a1 in mice with liver-specific deletion of *Fxr* ( $\Delta L$ ) but not in mice with intestinal deletion of *Fxr* ( $\Delta I$ E), indicating that activation of FXR in intestine but not in the liver mediates hepatic effects of GW4064 (21). These data are further supported by the pharmacokinetic properties of GW4064, which is characterized by a poor bioavailability (21). However, in conditions associated with hepatic steatosis different mechanisms are come into effect. Activation of FXR by the synthetic agonist GW4064 significantly improves plasma glucose and lipid levels in diabetic *db/db* mice (17, 18). Interestingly, blood glucose levels of both, nondiabetic wildtype and systemic *Fxr*  $-/-$  mice were reduced significantly after hepatic overexpression of constitutively active FXR by adenovirus-mediated gene transfer in the same study (17, 18). The present study under 1% cholesterol diet now clearly proves that lipid lowering FXR effects are exclusively mediated within the liver since the absence of hepatic FXR contributes to lipid accumulation independently of intestinal FXR. In accordance with previous data in genetic obesity models (17, 18), hepatic FXR similarly contributes to maintain normal serum cholesterol under a cholesterol diet. The finding that exclusively hepatic and not intestinal FXR deletion contributes to lipid accumulation under 1% cholesterol diet suggests that the observed effects are independent of intestinal Fgf15 induction. This is further supported by Fgf15 expression levels in our study which are unaltered in liver-specific (*Fxr*  $\Delta L$ ) mice compared *flox/flox* controls. These concepts are summarized in figure 6.

In conclusion, the present study clearly demonstrates that the principal site of protective FXR signalling against lipid accumulation is located in the liver since the absence of hepatic but not intestinal FXR contributes to lipid accumulation under cholesterol diet. In the absence of hepatic FXR elevated LXR expression can be observed together with the induction of lipogenic LXR-target genes such as *Scd-1* and *Fas*. As a mechanistic insight from this study, therapeutic effects of FXR agonists on fatty liver are attributable on one hand to their activation of bile acid transport and on the other hand to the inhibition of the lipogenic transcription factor LXR. Understanding these complex pathophysiological interactions will contribute to the generation of novel future treatment strategies for fatty liver disease.

## Acknowledgments

The authors thank Claudia Gottier, Sarah Mertens, Lia Hofstetter and Donata Dorbath for their excellent technical assistance. This work was supported by the *Swiss National Science Foundation* (SNF) grant 310000-122310/1 (to A.G.), and by the National Institutes of Health Grants DK031343-01 and P20-RR021940 (to G.L.G.).

## Abbreviations

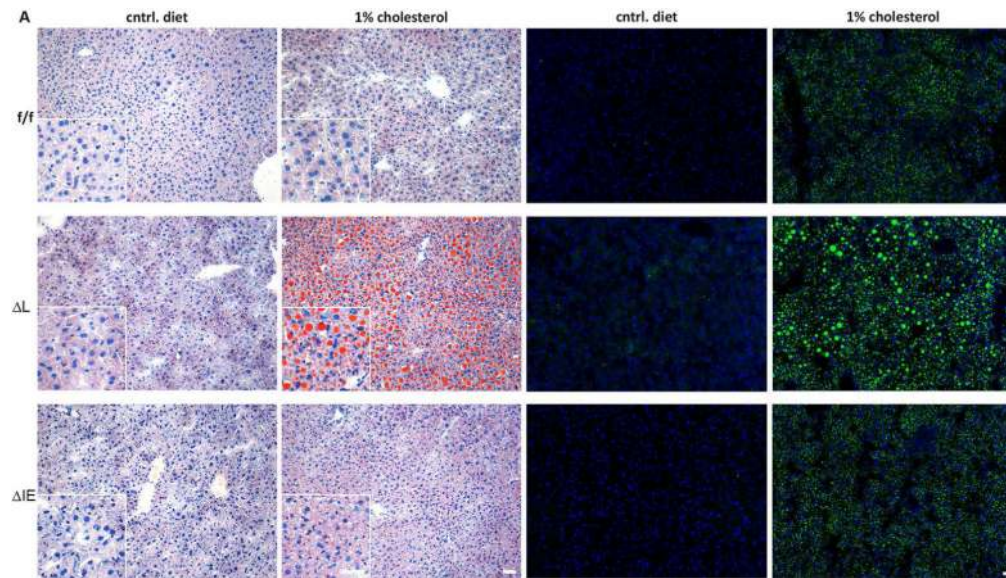
<b>BSEP</b>	bile salt export pump
<b>Cyp7a1</b>	cholesterol 7-alpha-hydroxylase
<b>CA</b>	Cholic acid
<b>CDCA</b>	Chenodeoxycholic Acid, Fas, fatty acid synthase

<b>FXR</b>	farnesoid X receptor/bile acid receptor
<b>HMGCoAR</b>	hydroxymethylglutaryl-Coenzyme A reductase
<b>Ibap</b>	ileal bile acid binding protein
<b>LXR</b>	liver X receptor
<b>NAFLD</b>	non-alcoholic fatty liver disease
<b>SCD-1</b>	Stearoyl CoA Desaturase-1
<b>SREBP-1c</b>	sterol regulatory element-binding protein isoform 1c
<b>SHP</b>	short heterodimer partner

## REFERENCES

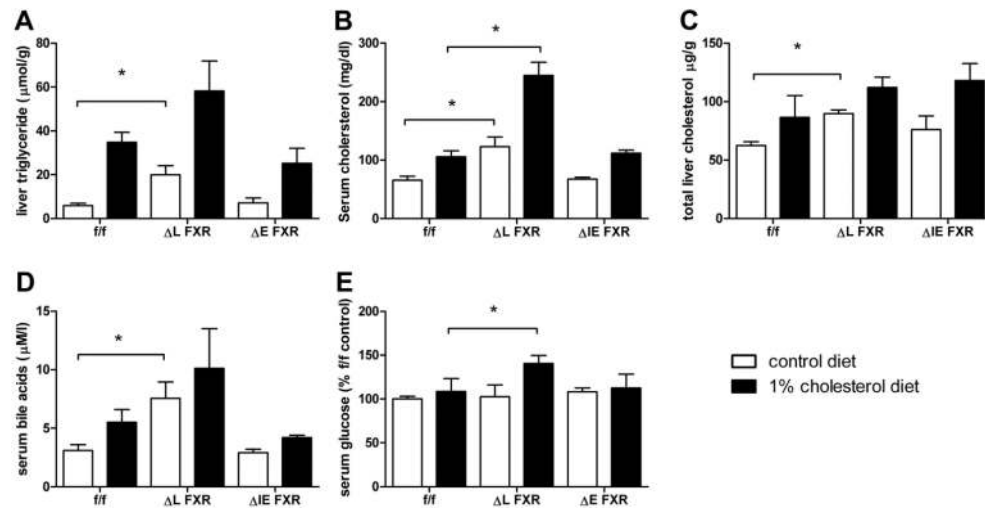
- Mendez-Sanchez N, Arrese M, Zamora-Valdes D, Uribe M. Current concepts in the pathogenesis of nonalcoholic fatty liver disease. *Liver Int.* 2007; 27:423–433. [PubMed: 17403181]
- Adams LA, Angulo P, Lindor KD. Nonalcoholic fatty liver disease. *Cmaj.* 2005; 172:899–905. [PubMed: 15795412]
- Angulo P. Nonalcoholic fatty liver disease. *N Engl J Med.* 2002; 346:1221–1231. [PubMed: 11961152]
- Stefan N, Kantartzis K, Haring HU. Causes and metabolic consequences of Fatty liver. *Endocr Rev.* 2008; 29:939–960. [PubMed: 18723451]
- Erickson SK. Nonalcoholic fatty liver disease. *J Lipid Res.* 2009; 50(Suppl):S412–416. [PubMed: 19074370]
- Stroeve JH, Brufau G, Stellaard F, et al. Intestinal FXR-mediated FGF15 production contributes to diurnal control of hepatic bile acid synthesis in mice. *Lab Invest.* 2010
- Fuchs M. Non-alcoholic Fatty liver disease: the bile Acid-activated farnesoid x receptor as an emerging treatment target. *J Lipids.* 2012; 2012:934396. [PubMed: 22187656]
- Adorini L, Pruzanski M, Shapiro D. Farnesoid X receptor targeting to treat nonalcoholic steatohepatitis. *Drug Discov Today.* 2012; 17:988–997. [PubMed: 22652341]
- Makishima M, Okamoto AY, Repa JJ, et al. Identification of a nuclear receptor for bile acids. *Science.* 1999; 284:1362–1365. [PubMed: 10334992]
- Geier A, Wagner M, Dietrich CG, Trauner M. Principles of hepatic organic anion transporter regulation during cholestasis, inflammation and liver regeneration. *Biochim Biophys Acta.* 2007; 1773:283–308. [PubMed: 17291602]
- Schmidt DR, Holmstrom SR, Fon Tacer K, et al. Regulation of bile acid synthesis by fat-soluble vitamins A and D. *J Biol Chem.* 2010; 285:14486–14494. [PubMed: 20233723]
- Bilz S, Samuel V, Morino K, et al. Activation of the farnesoid X receptor improves lipid metabolism in combined hyperlipidemic hamsters. *Am J Physiol Endocrinol Metab.* 2006; 290:E716–722. [PubMed: 16291572]
- Watanabe M, Houten SM, Wang L, et al. Bile acids lower triglyceride levels via a pathway involving FXR, SHP, and SREBP-1c. *J Clin Invest.* 2004; 113:1408–1418. [PubMed: 15146238]
- Lambert G, Amar MJ, Guo G, et al. The farnesoid X-receptor is an essential regulator of cholesterol homeostasis. *J Biol Chem.* 2003; 278:2563–2570. [PubMed: 12421815]
- Ma K, Saha PK, Chan L, Moore DD. Farnesoid X receptor is essential for normal glucose homeostasis. *J Clin Invest.* 2006; 116:1102–1109. [PubMed: 16557297]
- Sinal CJ, Tohkin M, Miyata M, et al. Targeted disruption of the nuclear receptor FXR/BAR impairs bile acid and lipid homeostasis. *Cell.* 2000; 102:731–744. [PubMed: 11030617]

17. Zhang Y, Lee FY, Barrera G, et al. Activation of the nuclear receptor FXR improves hyperglycemia and hyperlipidemia in diabetic mice. *Proc Natl Acad Sci U S A.* 2006; 103:1006–1011. [PubMed: 16410358]
18. Cariou B, van Harmelen K, Duran-Sandoval D, et al. The farnesoid X receptor modulates adiposity and peripheral insulin sensitivity in mice. *J Biol Chem.* 2006; 281:11039–11049. [PubMed: 16446356]
19. Geier A, Dietrich CG, Grote T, et al. Characterization of organic anion transporter regulation, glutathione metabolism and bile formation in the obese Zucker rat. *J Hepatol.* 2005; 43:1021–1030. [PubMed: 16139386]
20. Martin IV, Schmitt J, Minkenberg A, et al. Bile acid retention and activation of endogenous hepatic farnesoid-X-receptor in the pathogenesis of fatty liver disease in ob/ob-mice. *Biol Chem.* 2010; 391:1441–1449. [PubMed: 20868235]
21. Kim I, Ahn SH, Inagaki T, et al. Differential regulation of bile acid homeostasis by the farnesoid X receptor in liver and intestine. *J Lipid Res.* 2007; 48:2664–2672. [PubMed: 17720959]
22. Schmitt J, Benavente R, Hodzic D, et al. Transmembrane protein Sun2 is involved in tethering mammalian meiotic telomeres to the nuclear envelope. *Proc Natl Acad Sci U S A.* 2007; 104:7426–7431. [PubMed: 17452644]
23. Radin NS, Boulton AA, Baker GB, Horrocks LA. *Lipid Extraction. Lipids and Related Compounds.* 1998; 7:1–61.
24. Chiang JY. Regulation of bile acid synthesis: pathways, nuclear receptors, and mechanisms. *J Hepatol.* 2004; 40:539–551. [PubMed: 15123373]
25. Fuchs CD, Claudel T, Halilbasic E, Stojakovic T, Trauner M. Intrahepatic changes in bile acid composition protects Bsep (Abcb11) KO mice from hepatic inflammation in methionine choline deficient diet induced NASH. *Journal of Hepatology.* 2013; 58(Suppl.1):S32.
26. Li T, Chiang JY. Nuclear receptors in bile acid metabolism. *Drug Metab Rev.* 2013; 45:145–155. [PubMed: 23330546]
27. Chiang JY. Bile acids: regulation of synthesis. *J Lipid Res.* 2009; 50:1955–1966. [PubMed: 19346330]
28. Bechmann LP, Kocabayoglu P, Sowa JP, et al. Free fatty acids repress small heterodimer partner (SHP) activation and adiponectin counteracts bile acid-induced liver injury in superobese patients with nonalcoholic steatohepatitis. *Hepatology.* 2013; 57:1394–1406. [PubMed: 23299969]
29. Lehmann JM, Kliewer SA, Moore LB, et al. Activation of the nuclear receptor LXR by oxysterols defines a new hormone response pathway. *J Biol Chem.* 1997; 272:3137–3140. [PubMed: 9013544]
30. Fievet C, Staels B. Liver X receptor modulators: effects on lipid metabolism and potential use in the treatment of atherosclerosis. *Biochem Pharmacol.* 2009; 77:1316–1327. [PubMed: 19101522]
31. Peet DJ, Turley SD, Ma W, et al. Cholesterol and bile acid metabolism are impaired in mice lacking the nuclear oxysterol receptor LXR alpha. *Cell.* 1998; 93:693–704. [PubMed: 9630215]
32. Goldstein JL, Brown MS. Regulation of the mevalonate pathway. *Nature.* 1990; 343:425–430. [PubMed: 1967820]
33. Wang H, Chen J, Hollister K, Sowers LC, Forman BM. Endogenous bile acids are ligands for the nuclear receptor FXR/BAR. *Mol Cell.* 1999; 3:543–553. [PubMed: 10360171]
34. Schultz JR, Tu H, Luk A, et al. Role of LXRs in control of lipogenesis. *Genes Dev.* 2000; 14:2831–2838. [PubMed: 11090131]
35. Edwards PA, Kast HR, Anisfeld AM. BAREing it all: the adoption of LXR and FXR and their roles in lipid homeostasis. *J Lipid Res.* 2002; 43:2–12. [PubMed: 11792716]
36. Horton JD, Goldstein JL, Brown MS. SREBPs: activators of the complete program of cholesterol and fatty acid synthesis in the liver. *J Clin Invest.* 2002; 109:1125–1131. [PubMed: 11994399]
37. Jump DB, Botolin D, Wang Y, et al. Fatty acid regulation of hepatic gene transcription. *J Nutr.* 2005; 135:2503–2506. [PubMed: 16251601]
38. Wang YM, Zhang B, Xue Y, et al. The mechanism of dietary cholesterol effects on lipids metabolism in rats. *Lipids Health Dis.* 2010; 9:4. [PubMed: 20070910]



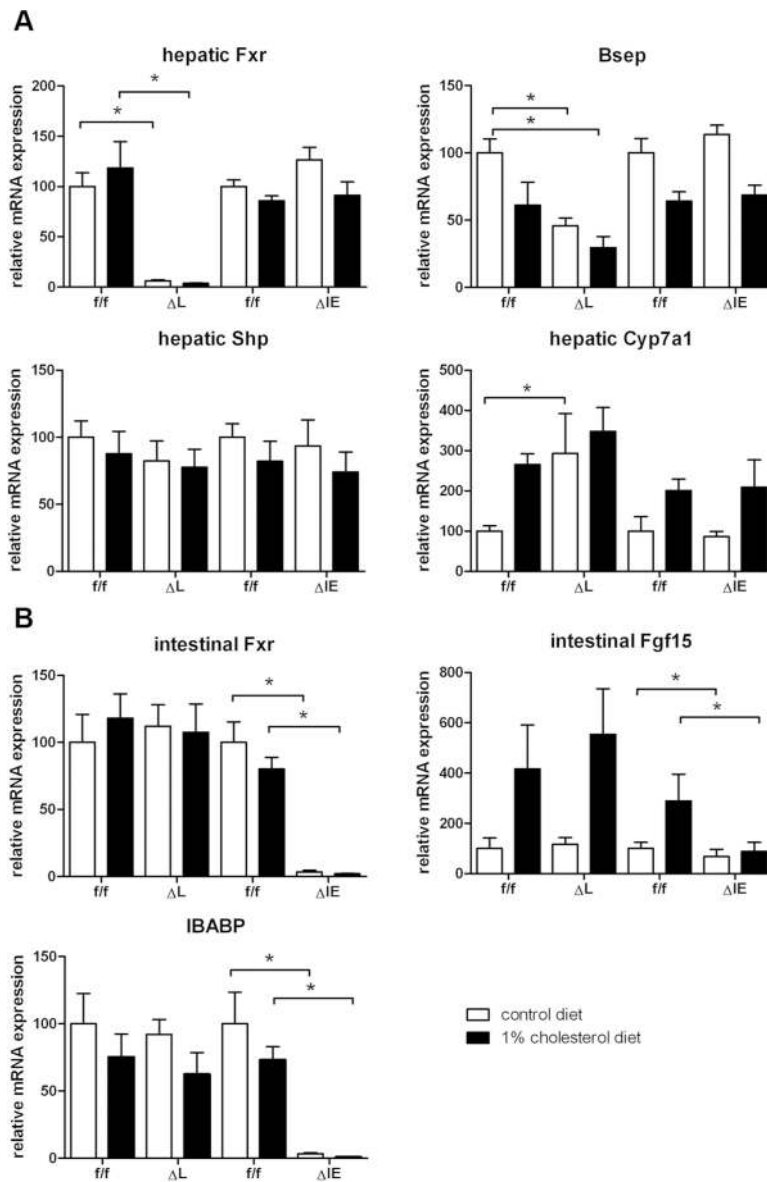
**Figure 1.**

Liver histology. Representative hematoxylin and Sudan III staining of *flox/flox*,  $\Delta L$  *Fxr* and  $\Delta IE$  *Fxr* knockout mice under control diet and 1% cholesterol diet (left panel). Representative BODIPY staining of *flox/flox*,  $\Delta L$  *Fxr* and  $\Delta IE$  *Fxr* knockout mice under control diet and 1% cholesterol diet are shown in a lower magnification (right panel). Massive lipid accumulation can be seen in  $\Delta L$  *Fxr* knockout mice under 1% cholesterol diet. Insert shows tissue in a higher magnification. Scale bars: 10  $\mu$ m.

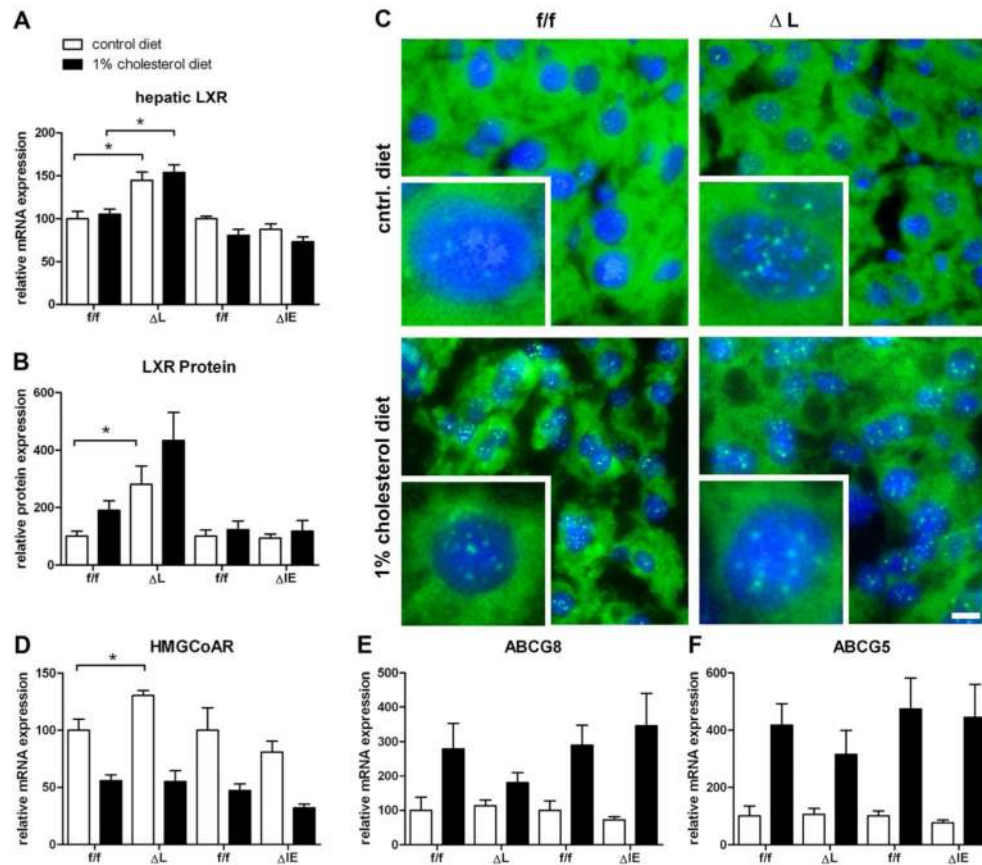


**Figure 2.**

Lipid content and serum parameters in organ-specific knockout animals. **A.** liver triglycerides **B.** serum cholesterol in mg/dl **C.** total liver cholesterol in  $\mu\text{g/g}$  **D.** total serum bile acids in  $\mu\text{M/l}$  and **E.** serum glucose in % of *flox/flox*,  $\Delta L Fxr$  and  $\Delta IE Fxr$  knockout mice under control diet and 1% cholesterol diet. Asterisk represents  $P < 0.05$  as determined by the Mann-Whitney U-test.

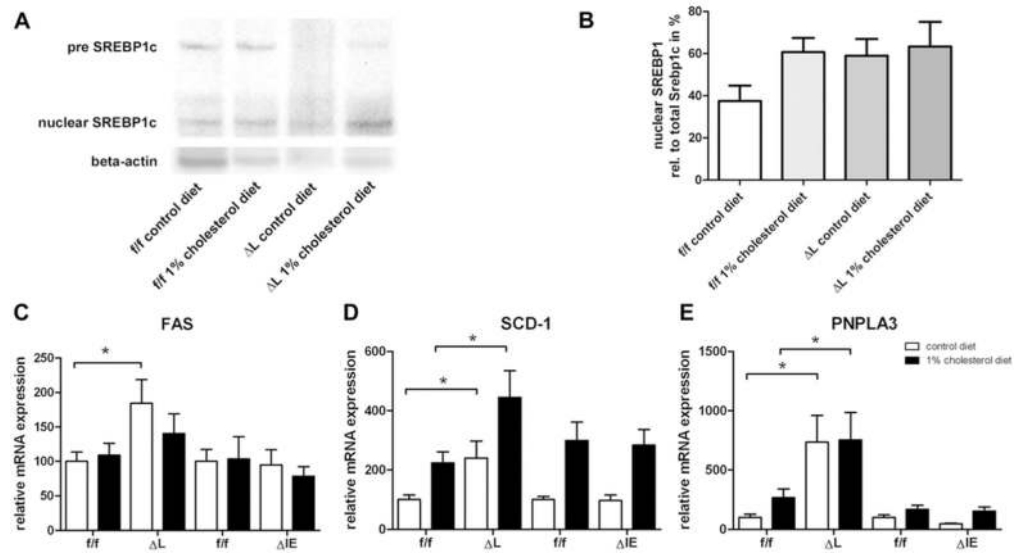


**Figure 3.** Relative quantification of the transcripts of nuclear receptors and their targets. RT-PCR was performed with RNA samples isolated from liver and ileum of *flox/flox*,  $\Delta L$  *Fxr* and  $\Delta IE$  *Fxr* knockout mice. **A.** hepatic genes were analysed: *Fxr*, *Shp*, *Cyp7a1* and *Bsep*. **B.** intestinal genes were analysed: *Fxr*, *Ibap* and *Fgf15*. Data represent means  $\pm$  SEM (n = 4-5). Asterisk represents  $P < 0.05$  as determined by the Mann-Whitney U-test.

**Figure 4.**

Liver X Receptor expression, localization and relative quantification of genes involved in cholesterol homeostasis. Respective liver tissue was used to isolate nuclear fractionations using the NE-PER Nuclear Extraction Reagents kit. **A.** hepatic LXR mRNA expression **B.** Nuclear LXR Protein content. Similar amounts of isolate nuclear fractionations from liver tissue, was analyzed. Nuclear LXR protein was determined using ELISA Kit for Liver X Receptor Alpha. LXR protein was normalized against total nuclear protein content. **C.** LXR immunohistochemistry. Increased nuclear localization in animals under 1% cholesterol diet. Increased localisation of LXR, is shown in ( $\Delta L$ ) *Fxr* knockout animals under standard diet. *flox/flox* littermates under the same treatment show lower nuclear LXR localisation. RT-PCR was performed with RNA samples isolated from liver of *flox/flox*,  $\Delta L$  *Fxr* and  $\Delta IE$  *Fxr* knockout mice for **D.** HmgCoAr, **E.** *Abcg5* and **F.** *Abcg8*. Data represent means  $\pm$  SEM (n = 4-5). Asterisk represents  $P < 0.05$  as determined by the Mann-Whitney U-test.



**Figure 5.**

Quantification of genes involved in lipogenesis. **A.** SREBP-1c protein expression was measured by western blot. Decreased concentration of high molecular weight (pre) SREBP1-c, results in increased lower molecular weight (nuclear) SREBP1-c, indicating SREBP1-c proteolytic activation. **B.** Densitometric quantification of Western blots was performed using Adobe Photoshop CS3, showing an increased SREBP1-c activation in  $\Delta L$  *Fxr* animal under control diet. RT-PCR was performed on RNA samples isolated from liver of *flox/flox*,  $\Delta L$  *Fxr* and  $\Delta IE$  *Fxr* knockout mice for **C.** Fas, **D.** Scd-1 and **E.** Pnpla3. Data represent means  $\pm$  SEM (n = 4-5). Asterisk represents  $P < 0.05$  as determined by the Mann-Whitney U-test.

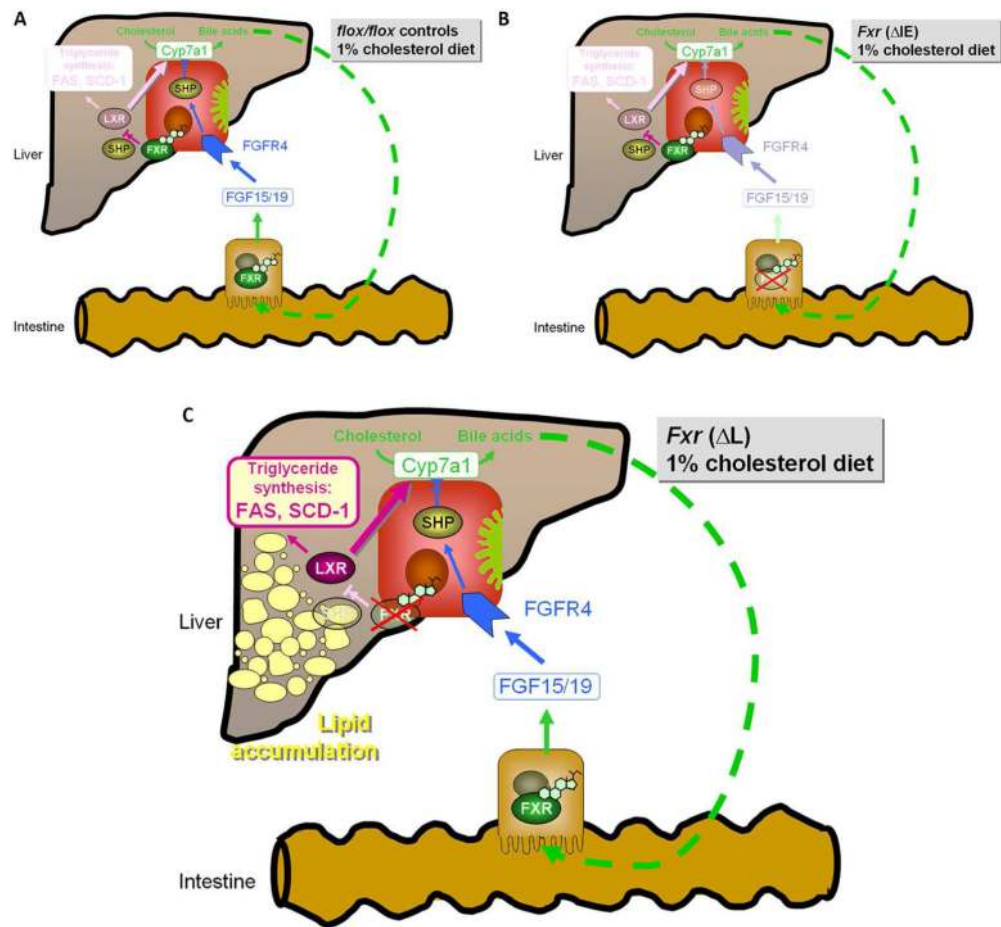


**Figure 6.**

Organ-specific protective effect of FXR against lipid accumulation. A. *flox/flox* controls B.  $\Delta$ IE *Fxr* knock out C.  $\Delta$ L *Fxr* knock out mice under 1% cholesterol diet. The principal site of protective FXR signalling against lipid accumulation is located in the liver since the absence of hepatic but not intestinal FXR contributes to lipid accumulation under 1% cholesterol diet. In the absence of hepatic FXR elevated LXR expression can be observed together with the induction of lipogenic LXR-target genes such as SCD-1. It could be suggested that the observed effects are independent of intestinal Fgf15 induction, as exclusively hepatic and not intestinal FXR deletion contributes to lipid accumulation under 1% cholesterol diet.

**Table 1**

Primer sequences used for real-time PCR

Primer	forward	reverse
Fxr	CTTGATGTGCTACAAAAGCTGTG	ACTCTCCAAGACATCAGCATCTC
Shp	CGATCCTCTTCAACCCAGATG	AGGGCTCCAAGACTTCACACA
Fgf15	GAGGACCAAAACGAACGAAATT	ACGTCCTTGATGGCAATCG
Cyp7a1	AGCAACTAAACAACCTGCCAGTACTA	GTCCGGATATTCAAGGATGCA
HMGCoAR	CTTGTGGAATGCCTTGTGATTG	AGCCGAAGCAGCACATGAT
Scd-1	CCGGAGACCCCTTAGATCGA	TAGCCTGTAAAAGATTTCTGCAAACC
Fas	TTCGGCTGCTGTTGGAAGTCAG	ACCCACCCAGACGCCAGTGTTTC
Pnpla3	ATCCCTCTTCTCTGGCCTA	ATGTCATGCTCACCGTAGAAAGG
IBABP	GGTCTTCCA GGAGACGTGAT	ACATTCTTTGCCAATGGTGA
BSEP	AAGCTACATCTGCCTTAGACACAGAA	CAATACAGGTCCGACCCTCTCT
LXR	GCTCTGCTCATTGCCATCAG	TGTTGCAGCCTCTCTACTGGA
$\beta$ -actin	TATTGGCAACGAGCGGTTCC	GGCATAGAGGTCTTTACGGATGTC
Taqman probes	Applied Biosystems ID	
Abcg5	Mm00446241_m1	
Abcg8	Mm00445980_m1	
$\beta$ -actin	4352341E	